# Progress Report No. 2

# MECHANISM OF THE PHOTOVOLTAIC EFFECT IN II-VI COMPOUNDS

National Aeronautics and Space Administration Lewis Research Center Cleveland, Ohio

October 1, 1967 - March 31, 1968

School of Engineering
Department of Materials Science
Stanford University
Stanford, California

Grant NGR-05-020-214

Report No. SU-DMS-68R-64

Principal Investigator

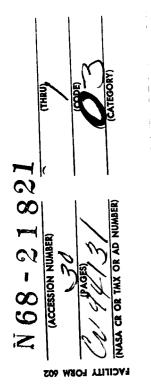
Richard H. Bube, Professor

Report Prepared by:

R. H. Bube

W. Gill

P. Lindquist





### SUMMARY

- FABRICATION AND MEASUREMENT OF Cu<sub>2</sub>S-CdS HETEROJUNCTION DIODES
   Current-voltage and capacitance-voltage measurements have been made
   on mesa diodes of Cu<sub>2</sub>S-CdS.
- 2. I-V CHARACTERISTICS

A variety of I-V characteristics are observed for the Cu<sub>2</sub>S-CdS diodes at room temperature. Values of the parameter multiplying kT in the exponential forward current expression lie between 1.1 and 1.3. An apparent barrier height of 0.6 eV was indicated from the I-V curves.

- 3. JUNCTION CAPACITANCE MEASUREMENTS
  - Theoretical expressions for highly asymmetrical heterojunctions are applied to experimental data to give a linear plot of  $C^{-1.25}$  vs V, with an indicated barrier height of 0.6 eV. These capacitance measurements would be consistent with a retrograde donor density profile, implying a copper concentration in the CdS depletion region which increases with distance into the CdS before finally decreasing.
- 4. EPITAXIAL GROWTH OF Cu<sub>2</sub>S on CdS

  A CdS crystal whose Cd (0001) face was exposed to a Cu<sup>+</sup> solution at 90°C for 24 hours showed a reacted layer about 115 microns thick.

  Distinct 6-fold symmetry was seen in x-ray back-reflection Laue photo-
- 5. OPTICAL MICROPROBE EXPERIMENTS
  - A. The technique of using a travelling light spot to determine minority carrier lifetimes is useful in the present problem.

graphs. The properties of the cell formed in this way were measured.

# Summary (Cont'd.)

- B. Values are available from the literature for typical minority carrier lifetimes and mobilities in CdS crystals.
- C. A microprobe has been constructed which forms an image on the crystal which is 20 microns long by 0.8 microns wide.
- D. The angle-lapped junction method is used for measuring diffusion lengths. Application to  $Cu_2S$ -CdS junctions indicates an electron diffusion length in the  $Cu_2S$  of less than 0.1 micron, a hole diffusion length in the CdS of 1.0 micron, a depletion layer width of 3.3 microns, and a hole lifetime of 2.7 x  $10^{-8}$  seconds in CdS.
- verse bias voltages. The magnitude of the effect increases with distance from the interface while the light spot is in the depletion region, and then decreases as the light is moved into the diffusion region. The measured gain was about 34. Of the two likely mechanisms, impact ionization of impurities or modulation of reverse leakage current, the latter seems most reasonable. The response time for the amplified photosignal was 200 microseconds.

# 1. FABRICATION AND MEASUREMENT OF Cu S-CdS HETEROJUNCTION DIODES

In order to arrive at a more complete understanding of the origin of the spectral response of photovoltage in Cu<sub>2</sub>S-CdS heterojunctions, it is necessary to obtain detailed information about the junction parameters such as depletion layer width, diffusion lengths, lifetimes of minority carriers, etc. A considerable amount of such information can be obtained by the analysis of current-voltage (I-V) characteristics and capacitance-voltage (C-V) curves. In order to minimize surface effects which cause a "soft" reverse characteristic, "mesa" structures are usually used.

Fig. 1 indicates the configuration of a typical mesa. A CdS crystal with an appropriately prepared surface is reacted in a Cu solution at 90°C for a prescribed time. The crystal sides are masked with black wax (Apiezon) so that only the surface of interest is exposed to the solution. After a Cu<sub>2</sub>S layer of thickness 10-50 microns has been formed, a layer of indium is evaporated onto the Cu2S surface. Small dots of black wax softened in trichloroethylene are then applied to the indium surface. The dots typically range in size from 0.5 - 1.0 mm in diameter. The crystal is then heated briefly at about 60°C to drive off the trichloroethylene and bond the black wax securely to the surface. Etching of the mesas is carried out by first dipping the crystal in concentrated HC & to dissolve the indium. The Cu2S is then removed by KCN, followed by another dip in HCL to remove a layer of CdS and so isolate the junction region, as shown in Fig. 1. The crystal specimen, containing up to 15 of these mesas, is mounted in a holder which makes an ohmic gallium-indium contact to the CdS base and a tungsten point contact to the indium layer on a selected mesa. Room temperature capacitance and I-V measurements are made in this holder in the dark and with illumination.

### 2. I-V CHARACTERISTICS

A variety of I-V characteristics have been observed for the  $\operatorname{Cu}_2\operatorname{S}$ -CdS diodes. The curves are usually measured with a Tektronix type 575 transistor curve tracer. This is a convenient way to observe the overall features of the curve quickly, but for precise measurements at very low current densities (where tunneling effects become dominant) a point-by-point measurement must be made. The "softness" of the reverse characteristic of these diodes appears to be related to the conductivity of the CdS base. This is in accord with the expression for the reverse current given by  $\operatorname{leCan}^{(1)}$ :

$$I_{R} = q \frac{A D_{p}}{W} M \left( 1 + \frac{1}{\alpha'} \right) p_{N} + V_{R} / r_{L}$$
 (1)

in which

$$M = \left[1 - \left(\frac{v_R}{v_{Av}}\right)^n\right]^{-1} \tag{2}$$

is the avalanche multiplication factor. For a given value of reverse bias,  $\mathbf{V}_R$ , M is very sensitive to changes in majority carrier concentration in the base,  $\mathbf{n}_N$ , increasing with increasing  $\mathbf{n}_N$ .  $\mathbf{r}_L$  is the surface leakage resistance, and  $\overline{\alpha}'$  is the "base current amplification factor" which is proportional to  $\mathbf{n}_N^{-1}$  and includes surface effects. Thus  $\mathbf{p}_N/\overline{\alpha}'$  is independent of  $\mathbf{n}_N$ , so that one term of (1) increases with  $\mathbf{n}_N$  as M. q is the electronic charge, A is the junction area,  $\mathbf{D}_p$  is the diffusion coefficient for holes in n-type material, and W is the width of the space-charge region.

Fig. 2 shows the room temperature I-V characteristic for a mesa designated 3-95-A. The CdS substrate has a resistivity of 0.8 ohm-cm. The crystal was immersed for 11 hours in a CuCl solution at 85-90°C, resulting in a layer approximately 50 microns thick. The resistivity of the layer

was measured by the four-point probe technique and found to be about  $4.5 \times 10^{-4}$  ohm-cm. An x-ray Debye-Scherrer powder pattern was taken from a portion of the layer, using a 114.6 mm camera and exposing for 8 hours with copper K radiation. The table below shows the analysis of the pattern.

Analysis of X-Ray Powder Pattern of Cu-S Layer from Diode 3-95-A

Line No.	Intensity	<u>d, A</u>	12-227* Cu <sub>2</sub> S	6 <b>-</b> 0464 CuS	9-64 Cu <sub>9-x</sub> S <sub>5</sub>	12-205 Cu <sub>1.96</sub> S
1	vvw?	8.007	8.51	8.18	-	
2	VVw?	6.753	6.40	-	-	-
3	VVw?	6.063	-	-	-	-
4	M	4.129	4.27	-	-	4.29
. 5	W	3.718	3.73	-	-	3.748
6	M	3.216	3.181	3.220	3.21	3.191
7	vs	3.034	3.051	3.048	3.05	3.035
8	VS	2.889	2.882	-		2.889
9	S	2.714	2.724	2.724	-	2.688
10	W	2.312	2.328	2.317	-	2.316
11	VS	1.890	1.895	1.896	-	1.870

## \* ASTM Card File number

The I-V characteristic shown in Fig. 2 was measured with the tungsten point in direct contact with the Cu<sub>2</sub>S surface. It was found that the series resistance was very high, and that it varied from point to point on the mesa surface. This may be due to cracks in the Cu<sub>2</sub>S layer parallel to the surface. (The x-ray pattern showed considerable asterism in the forward-reflection region, indicating that the Cu<sub>2</sub>S is highly strained.)

Fig. 3 gives plots of the forward characteristic of the diode, both "as-measured" and after correction for series resistance, which in the case

shown was 780 ohms. A second corrected plot is shown for another measurement, in which the point contact was located in another area and a different value of series resistance (300 ohms) was obtained. These straightline plots can be represented (for  $V \gg kT/q$ ) by

$$I = I_o e^{qV/AkT} . (3)$$

The values of A obtained from these characteristics are 1.13 and 1.29. These values, while reasonable, are not considered of too great significance at this point, since only one decade of current is involved and measurements have not as yet been made as a function of temperature. (A should be independent of temperature, according to the physical model which results in equation (3).) A value of A greater than one indicates that recombination in the space-charge region is important. These forward I-V characteristics resulted in an apparent "barrier height" of about 0.6 volt when the linear portion (on a linear plot) was extrapolated to I = 0 (see Fig. 2). This is in contrast to the generally reported value of 0.8 volt for the Cu<sub>2</sub>S-CdS junction.

### 3. JUNCTION CAPACITANCE MEASUREMENTS

The measurement of junction capacitance as a function of applied DC bias and intensity and wavelength of illumination is a convenient way to acquire information about the width of the space-charge region and the charge density profile near the edges of this region. For a heterojunction, the capacitance per unit area according to the Schottky theory is (2)

$$\frac{C}{A} = \left(\frac{q \epsilon_1 \epsilon_2 N_1 N_2}{2(\epsilon_1 N_1 + \epsilon_2 N_2)}\right)^{\frac{1}{2}} (V_D - V)^{-\frac{1}{2}}$$
(4)

where  $V_D$  is the diffusion voltage (barrier voltage) and  $\varepsilon_1$ ,  $\varepsilon_2$  are the dielectric constants of the two materials. The expression above holds only for the case of a constant space-charge density across the depletion region. In practice, deviations from this "ideal" behavior are often found, i.e., plots of  $C^{-2}$  vs V are curved. Anderson<sup>(3)</sup> has shown that for highly asymmetrical (p<sup>+</sup>-n) heterojunctions, if the relationship

$$C = C_1 / (V_D - V)^{\alpha}$$
 (5)

holds over a range of applied bias, then the net donor density  $N_D$  -  $N_A$  as a function of distance from the metallurgical junction, x, is given by

$$(N_D - N_A) (x) = \frac{1}{\alpha} \frac{\epsilon}{q} \left(\frac{1}{x_o}\right)^2 \left(\frac{x}{x_o}\right)^{-[2-(1/\alpha)]}$$
 (6)

where x =  $x_0$  for  $V_D$  - V = 1.  $\varepsilon$  is the dielectric constant for the more lightly doped material (CdS). The obvious implication of the above expression is that for  $\alpha > \frac{1}{2}$ , the net donor concentration <u>decreases</u> with increasing x, i.e., a "retrograde" impurity distribution.

Fig. 4 presents capacitance-voltage data for diode 3-95-A. The value of the barrier voltage  $V_{\rm D}=0.6$  volt was taken from the measured I-V characteristic. It was necessary to correct the capacitance data for the effect of large series resistance (780 ohms for the case shown). If  $C_{\rm eq}$  and  $R_{\rm eq}$  are the measured values of capacitance and equivalent parallel resistance, and  $C_{\rm p}$ ,  $R_{\rm p}$ , and  $R_{\rm s}$  are the parameters of the series-parallel representation of the diode, then the corrected capacitance  $C_{\rm p}$  is given by

$$C_{p} = \frac{C_{eq}}{\left(1 - \frac{R_{s}}{R_{eq}}\right) (1 - \delta R_{s})}$$
 (7)

where

$$\delta = \frac{1 + R_s^2 \gamma}{R_{eq}} - R_s \gamma \tag{8}$$

and

$$\gamma = \omega^2 c_{eq}^2 / \left(1 - \frac{R_s}{R_{eq}}\right)^2$$
 (9)

The difference between  $C_{eq}$  and  $C_{p}$  is appreciable only for large  $R_{s}$  as in the case under consideration. The log C vs. log V plot in Fig. 4 is curved and should be analyzed in segments, each having its own slope. However, a slope of -0.8 fits the curve reasonably well, as shown. Thus a plot of  $C^{-1/0.8} = C^{-1.25}$  vs V should be roughly linear. This plot is given in Fig. 5. It is seen that the extrapolation gives  $V_{D} \approx 0.6$  volt, in agreement with the I-V measurement.

The conclusion drawn from these capacitance measurements is that a "retrograde" donor density profile may be involved, which would imply a copper concentration in the CdS depletion region which increases with distance into the CdS before finally decreasing. It is hoped that an independent experiment will be able to check this in the near future. It should be pointed out that similar capacitance data have now been observed for a number of diodes. One indication that such an unusual phenomenon may be occurring is the work by Hill (4) which showed that a "backward" junction may be produced by long-time, high temperature heat treatments of Cu<sub>2</sub>S - CdS cells.

### 4. EPITAXIAL GROWTH OF Cu2S ON CdS

Epitaxial growth of  $Cu_2S$  on single crystal CdS substrates has recently been reported in the literature (5). This experiment has been duplicated in this laboratory. A CdS crystal whose Cd (0001) face was exposed to a  $Cu^+$  solution at  $90^{\circ}C$  for 24 hours showed a reacted layer about 115

microns thick. X-ray back-reflection Laue photographs showed a pattern with distinct 6-fold symmetry, proof of an epitaxial relationship of the Cu<sub>2</sub>S with the CdS substrate. The layer was sufficiently thick so that no X-radiation penetrated through to the CdS.

Fig. 6 presents the backwall spectral response of short-circuit photocurrent for this specimen (designated 24-C). No heat treatment was given to the cell prior to measurement. This curve is comparable to those of the best single crystal cells made in this laboratory, even with heat treatment. The epitaxial relationship is therefore considered to be an important factor in promoting good spectral response characteristics in a single crystal cell.

Four-point probe measurements on the  $Cu_2S$  layer indicated a resistivity of 0.0032 ohm-cm. This value is somewhat higher than those generally reported for degenerate  $Cu_2S$ . This measurement together with the fact that it was quite difficult to make good ohmic contact to the layer suggested that the layer was indeed non-degenerate, possibly due to the presence of compensating  $Cd^{++}$  ions on  $Cu^{+}$  lattice sites.

#### OPTICAL MICROPROBE EXPERIMENTS

### A. Introduction

Morton and Haynes first proposed using a travelling light spot as a probe to determine the minority carrier diffusion length and hence lifetime. The technique has become a standard one for the measurement of minority carrier lifetimes in germanium (6-8) where the lifetimes are long. We give a brief analysis of the problem to show how light probe data can give a direct measure of the diffusion length from which the lifetime can be calculated.

We write the continuity equation for minority carriers (e.g., holes in n-type material)

$$\frac{\mathrm{dp}}{\mathrm{dt}} = G - \frac{P - P_0}{\tau_p} + \frac{1}{q} \nabla \cdot J_p$$
 (10)

where

$$J_{p} = q \mu_{p} p E + q D_{p} \nabla p . \qquad (11)$$

Substituting equation (11) into (10) and considering steady state conditions in one dimension leads to

$$G - \frac{p - p_0}{\tau_p} + \mu_p E \frac{dp}{dx} + \mu_p p \frac{dE}{dx} + D_p \frac{d^2p}{dx^2} = 0$$
 (12)

where G is the rate of hole production by light. For a small light spot G is assumed to be zero everywhere except at x = 0. Also since we are dealing with minority carriers, space charge neutrality can be assumed and equation (12) reduces to

$$-\frac{\Delta p}{\tau_p} + p_p \frac{d^2 \Delta p}{dx^2} = 0 \tag{13}$$

where  $\Delta p = p - p_0$ . Equation (13) has the solution

$$\Delta p = (\Delta p)_{x=0} e^{-x/L} p \tag{14}$$

where  $L_p = \sqrt{\frac{D_p \tau}{p p}}$  is the hole diffusion length.

A pn-junction is a convenient collector for the diffusing minority carriers. If the light spot is positioned some distance x from the space charge region on the n side of a p-n junction, the photocurrent collected by the junction will be proportional to  $\Delta p$ . Thus a plot of  $\ln$  I versus x should yield a straight line with slope -  $\frac{1}{L}$  . If the minority carrier mobility  $\mu$  is known, then the lifetime can be calculated using the

Einstein relation.

The travelling light spot technique becomes difficult in materials where the diffusion lengths are of the order of microns. However, by using extremely small light spots, highly absorbed light, and angle lapped junctions, diffusion lengths less than a micron may be measured (9-11).

# B. Application to CdS-Cu<sub>2</sub>S Heterojunctions

In the CdS-Cu<sub>2</sub>S heterojunctions capacitance measurements indicate barrier widths in the range of 1 to 3 microns. Because of the high conductivity of the p type  $Cu_2S$  layer almost the entire barrier width occurs on the CdS side of the junction. The minority carrier lifetime  $\tau_p$  in pure CdS crystals has been measured  $^{12}$  and lies in the range of  $1\text{-}3\text{x}10^{-7}$  seconds. The room temperature mobility was also determined by these authors to be  $^{15}$  cm $^{2}$ /V-sec. Thus one might expect a diffusion length of a few microns for holes diffusing to the junction on the CdS side. On this basis it was felt that a precise microprobe technique would allow direct determination of the diffusion length on the CdS side and also be a useful probe of the space charge region in the junction.

In the following sections the microprobe which has been constructed is described, and some preliminary measurements and results are presented.

### C. Microprobe Description

A schematic of the microprobe is shown in Fig. 7. The collimated beam of a 150-watt xenon arc is passed through a monochromator or suitable filters and illuminates a slit 0.4 mm wide by 10 mm long. The light passing through the slit is chopped at 114 cps, passes through lens  $L_1$  and into the side port of a metallurgical microscope. The light is totally reflected by a  $90^{\circ}$  prism and imaged on the sample by the microscope objec-

tive lens. The size of the image is determined by the focal length of the microscope objective and for a given lens L2 by the distance d from the slit to  $L_2$ . As the prism only obscures half the microscope field the sample can be viewed through the microscope in the usual way. To keep the beam divergence angle  $\varphi$  as small as possible a long focal length objective (10.25 mm) is used. The slit is reduced a factor of 50 by lens  $L_{\rm l}$  and another factor of 10 by the objective for an overall demagnification of 500X. Thus a line image is formed on the sample 20 microns long by 0.8 microns wide. The width of the image is very near the theoretical resolution limit which for 5000 A light is 0.6 microns. To decrease further the light spot would require a larger aperture objective lens resulting in a divergence angle >90° making focusing extremely critical. The sample is held on a mount which can be rotated to make the projection of the junction plane parallel to the line image. The entire shielded sample holder is mounted on a calibrated precision motion which allows accurate positioning perpendicular to the line image to better than  $\pm \frac{1}{2}$  micron. Motion in the two other orthogonal directions is made with a standard micromanipulator.

The photocurrent generated in the sample is detected by a PAR HR-8 Lock-in Amplifier using a low input impedance ( $100\Omega$ ) Type B preamplifier. A reference signal from the light chopper is also fed into the lock-in amplifier. Signal currents as small as  $10^{-11}$  amp can be measured with reasonable signal-to-noise ratios which is found to be adequate sensitivity for the photocells being measured.

External bias voltage can be applied to the sample from a battery power supply. A large capacitor (200 µf) in the circuit is used to block

dc currents from passing through the lock-in amplifier.

# D. Preliminary Measurements and Results

Because the diffusion lengths in the system CdS-Cu<sub>2</sub>S are expected to be small the angle-lapped junction method for measuring diffusion lengths is used. Fig. 8 shows the geometry of the samples in this experiment. The bevel angle  $\theta$  was chosen to give maximum spatial resolution to the experiment keeping in mind that at very small angles interface roughness becomes a serious problem. In the angle-lapped method highly absorbed light must be used. Minority carriers created very near the surface diffuse in the y-direction to the edge of the space-charge region where they are collected by the field across the junction. Moving the light spot in the x-direction results in a corresponding increase in the distance y measured normal to the junction by the amount

$$y = x \sin \theta . (15)$$

Since the number of carriers reaching the space-charge region is given by

$$\Delta p = (\Delta p)_{o} e^{-\dot{y}/L}$$
(16)

and the decrease in light intensity is approximately given by

$$I = I_0 e^{-\alpha y} , \qquad (17)$$

the ultimate limit on diffusion lengths which are measurable depends on the absorption coefficient. For CdS the maximum absorption coefficient is ( $\lambda < 4800 \text{ A}$ ) 8.5 x  $10^4 \text{ cm}^{-1}$ . (13) Since to measure the diffusion length by this method requires  $\alpha > \frac{1}{L}$  we see that the minimum measurable diffusion length is ( $L_p$ ) min  $\approx 3 \left(\frac{1}{\alpha_{max}}\right)^p = 3.6 \times 10^{-5} \text{cm}$ . For a 5° bevel angle, a motion

of 4 microns in the x-direction would correspond to  $(L_p)_{min}$  in the y-direction. As the sample can be easily positioned to within  $\frac{1}{2}$  micron a  $5^{\circ}$  angle is used. A few samples have also been bevelled at  $2^{\circ}$  when examining the  $Cu_2S$  side of the junction.

Fig. 9 is a plot of the short circuit photocurrent as a function of light spot position. The x=0 position was taken to be the visible interface between the CdS and the  $Cu_2S$  observed through the microscope at X200 magnification. The photocurrent is seen to increase sharply at the interface, remain nearly constant over a 40-micron distance and then to decrease exponentially falling at the rate of 1/e per twelve microns. Similar results were obtained in two other samples.

The interpretation of the data is that as the light beam crosses x = 0 pair generation takes place in the space-charge region. The internal field separates electrons and holes which flow to the n and p sides respectively. At x = 40 microns the light spot is at the edge of the space-charge region in the CdS and the depletion layer width  $W = 40 \sin 5^{\circ} = 3.3$  microns. At this point the entire current contribution is due to holes. As the light spot is moved further from the junction the only current is due to hole diffusion through a distance y to the edge of the space-charge region. The diffusion length  $L_p$  determined from the slope of the  $\ln I_{sc}$  versus x curve is 12 sin  $5^{\circ} = 1.0$  micron.

Similar measurements were made on the  $Cu_2S$  side of a junction by bevelling the opposite side of a crystal to obtain a wedge shaped region of  $Cu_2S$ . The results are shown in Fig. 10 for a bevel angle of  $2^{\circ}$ . The current falls off on the  $Cu_2S$  side extremely rapidly, decreasing by 1/e in about 3 microns corresponding to y = 0.1 microns. For 4800 A light  $\alpha =$ 

10<sup>5</sup>cm<sup>-1</sup> in Cu<sub>2</sub>S which means that the light penetration falls off by 1/e in 0.1 microns. We conclude that the electron diffusion length in the Cu<sub>2</sub>S is less than 0.1 microns and is not measurable by this technique. It may be noted that the depletion width is also very narrow on the Cu<sub>2</sub>S side as expected from its high conductivity.

From the data on the diffusion length in CdS, the hole lifetime can be obtained using  $L_p=\sqrt{D_p\tau_p}$  and the Einstein relation  $D_p=\mu_p\frac{kT}{e}$ . Using Spear's value of  $\mu_p$  = 15 cm²/v-sec results in  $\tau_p$  = 2.7 x 10 $^{-8}$  seconds.

# E. Voltage Bias Experiments and Minority Carrier Amplification

While investigating the effect of voltage bias on the depletion width W interesting minority carrier current amplification has been observed under small reverse bias. The effect is shown in Fig. 11 where in photocurrent is plotted as a function of reverse bias for sample CdS(C2). A number of curves are plotted corresponding to different positions of the light spot relative to the CdS-Cu<sub>2</sub>S interface. At the 40 micron position an increase in the measured photocurrent by a factor of 2000 was observed. The magnitude of the effect is seen to increase with distance from the interface while the light spot is in the space-charge region and then decreases as the light is moved into the diffusion region at the 50 and 60-micron positions. This suggests that the effect is due to the hole current and depends on the fraction of the depletion layer traversed by the photo-injected holes. Fig. 12 is a linear plot of the same effect over a wider bias range for white light incident at 40 microns from the interface. The dark current is also plotted for this cell.

To determine whether the large increase in photocurrent under reverse bias was solely due to increased collection efficiency of the junction due to the applied field separating the photo-excited charge pairs, the total photon flux incident on the sample was measured. For the wavelengths used the photon flux was found to be 1.3 x  $10^{12}$  photons/second. As the maximum gain expected in a photodiode is unity, this photon flux would at most give rise to a photocurrent of 2.1 x  $10^{-7}$  amperes. With the light spot at the 40-micron position and a reverse bias of 3 volts the measured photocurrent was 7.2 x  $10^{-6}$  amp or 34 times the unit gain current neglecting reflection and recombination losses entirely. It is apparent that a very substantial amount of minority carrier current amplification is occurring.

Avalanche multiplication is ruled out as a possible mechanism because of the low applied voltages at which the phenomenon is observed. Impact ionization of impurities and modulation of reverse leakage current are considered the most likely mechanisms. Measurement of the amplification effect and dark current as functions of reverse bias on several samples leads us to favor the modulation of leakage current as the mechanism responsible for the effect. This conclusion is due to the correlation observed between the amplification effect and the dark current for several samples. This correlation is shown for two samples in Fig. 13. Minority current amplification in non-ideal p-n junctions is treated in a paper by Stafeev (15). Basically the leakage current serves as a source of electrons which may be injected from the p-side of the junction to compensate the space charge of the light-injected holes. If no hole trapping occurs in the depletion region, current gain of  $1+\left(\frac{\mu_n}{\mu_p}\right)$  or about 14 is possible for If hole trapping does occur even larger gains are possible analogous to the photoconductive gain in sensitized crystals. The saturation behavior is not understood at present, but at the high dark current densities at

which saturation occurs increased recombination and higher junction temperature may be responsible for the decreased amplification at larger reverse bias.

If hole trapping is responsible for the large observed current gains, optical quenching of the gain might be expected. Preliminary quenching experiments with 0.9 micron light show no quenching, but more thorough investigation of this possibility is being undertaken. The response time of the amplified photosignal has been measured by measuring rise and decay times for pulsed light. The response time is found to be about  $2 \times 10^{-4}$  seconds.

# WORK PLANNED FOR NEXT REPORT PERIOD

During the next report period, efforts will be directed toward the following:

- (1) Improvement of the chemical dipping technique.
- (2) Improvement of methods for fabricating mesa diodes.
- (3) More precise measurements of C-V and I-V curves.
- (4) A search for additional evidence for a retrograde copper profile in CdS, a clarification of its origin, and determination of its relation to the photovoltaic effect.
- (5) Measurements of capacitance and I-V curves at various temperatures down to 77°K.
- (6) Clarification of the band diagram of the CdS-Cu2S heterojunction.
- (7) Study effect of post-dipping heat treatment on the depletion width W and the hole diffusion length  $L_p$ .
- (8) Further study of minority carrier amplification effect. It may be possible to use this effect to study hole trapping in the depletion region.
- (9) Use an intense auxiliary light source in conjunction with the microprobe to study possible bias light effects on a microscopic scale.
- (10) Extend the microprobe measurements to CdSe and ZnS cells.

### REFERENCES

- C. leCan, K. Hart, and C. deRuyter, <u>The Junction Transistor as a Switch-ing Device</u>, Reinhold Publishing Corp., New York, 1962, pp. 40-42.
- 2. J. P. Donnelly and A. G. Milnes, IEEE Trans. ED-14, 63 (1967).
- 3. R. L. Anderson and M. J. O'Rourke, IBM Journal, July, 1960, p. 264.
- 4. E. R. Hill and B. G. Keramidas, Rev. Phys. Appl. 1, 189 (1966).
- 5. J. Singer and P. A. Faeth, Appl. Phys. Let. 11, 130 (1967).
- 6. F. S. Goucher, Phys. Rev. 81, 475 (1951).
- 7. L. B. Valdes, Proc. I.R.E. 40, 1420 (1952).
- 8. F. S. Goucher et al., Phys. Rev. <u>81</u>, 637 (1951).
- 9. G. Jungk and H. Menninger, Phys. Stat. Sol. 5, 169 (1964).
- 10. M. H. Norwood and W. G. Hutchinson, Sol. State Electronics 8, 807 (1965).
- 11. K. L. Ashley and J. R. Biard, IEEE Trans. El. Dev. ED14, 429 (1967).
- 12. W. E. Spear and J. Mort, Proc. Phys. Soc. 81, 130 (1963).
- 13. D. Dutton, Phys. Rev. <u>112</u>, 785 (1958).
- 14. V. I. Stafeev, Sov. Phys. Tech. Phys. 14, 2037 (1957).

# FIGURE CAPTIONS

	$\cdot$
Figure 1	Configuration of a Cu <sub>2</sub> S-CdS mesa diode
Figure 2	I-V characteristic of mesa 3-95-A at room temperature
Figure 3	Forward characteristic of mesa 3-95-A at room temperature
Figure 4	Log C - log V plot for mesa 3-95-A: (a) As measured, (b) Corrected for series resistance
Figure 5	C-V plot for mesa 3-95-A (capacitance values corrected for series resistance)
Figure 6	Backwall spectral response of photocurrent for epitaxial Cu <sub>2</sub> S cell 24-C (not normalized for monochromator output)
Figure 7	Schematic of the microprobe
Figure 8	Geometry of the angle-lapped junctions
Figure 9	Short-circuit photocurrent as a function of light spot position for the CdS side of a junction
Figure 10	Short-circuit photocurrent as a function of light spot position for the $\mathrm{Cu_2}\mathrm{S}$ side of a junction
Figure 11	Photocurrent as a function of reverse bias voltage for probe positions numbered (1) through (5) on Fig. 9
Figure 12	Photocurrent and dark current versus reverse bias for sample CdS(C2)
Figure 13	Photocurrent and dark current versus reverse bias for two samples showing correlation of the current multiplication with leakage current

